

Limitations and Comparisons of Small Signal Modelling Techniques in Converter Dominated Medium Voltage Networks

University of Strathclyde ¹
16 Richmond St, Glasgow
G1 1XQ, Scotland

Scottish Power Energy Networks ²
320 St Vincent Street, Glasgow
G2 5AD, Scotland

sophie.coffey@strath.ac.uk

Sophie Coffey¹, Sam Harrison¹, Agustí Egea-Álvarez¹, Cornel Brozio²

Keywords

«Modelling», «Virtual Synchronous Machines», «Small-Signal», «Grid-Forming», «Distributed Generation»

Abstract

Grids are seeing changing SCRs, due to increased power converter penetration. This paper assesses several common small signal modelling techniques of varying computational complexity for their accuracy. Each model is tested for its accuracy limitations in response to a power disturbance for varying grid SCRs and X/R ratios and controller damping for distribution networks.

Introduction

The power system has seen significant changes over the last few decades as traditional fossil fuel power plants are being phased out and replaced with converter-based generation resources [1]. Traditional generation sites use synchronous machines to create a stiff voltage source, however, grids are now seeing converter dominated networks, which bring their own problems, with new device dependent and control interactions emerging [2]. Additionally, the short circuit ratio (SCR) is increasingly differing at points across the grid, and so the effect of SCR on model accuracy needs to be reviewed. Furthermore, the distribution network operators (DNOs) are seeing more renewable generation integrated into the distribution grid, instead of transmission grids, at a medium voltage level [3]. Distributed grids have a much lower X/R ratio compared to transmission grids [4], and so the effect of changing X/R ratios on model accuracy should also be investigated.

Utilisation of extensive large signal EMT models and small signal models can provide in depth information regarding power system stability and interactions [2] [1]. However, in

some instances they may be more detailed than is required, impractical to implement when there are many converters, and computationally intensive [5], [6].

In standard power networks, sub-synchronous oscillations (SSO) have been caused by interactions with the generator rotors, in series compensated transmission lines [7]. The swing equation has been commonly used to model synchronous machines connected to the grid, and to represent the interaction of the torsional modes causing the SSOs [7]. The new converter induced interactions require varying resolution of models to fully understand stability [8] [5] in the ever-changing grid of differing SCR and X/R levels.

Several instances of sub-synchronous oscillations that have caused stability issues to the grid, were not predicted or could not be modelled [9]. As such, understanding the limitations of (and suggesting improvements to) existing modelling techniques is vital. It has long been discussed in the literature [10], [11], these limitations, and the detail of information required in the model to accurately represent stability, transients and oscillations.

Consequently, this paper offers an insight into the limitations of commonly used modelling approaches from a small-signal perspective. The full detailed small signal [12], the Jacobian [13], and the classical models [7] will be assessed for accuracy compared to the full nonlinear EMT model. The effect of the SCR, damping ratio, and X/R ratio of the grid on the model accuracy will be investigated for each modelling method. The results of this paper act as motivation in the development of an improved modelling method for converter dominated networks to reduce the computational expense and the complexity of sub synchronous oscillation studies.

System Under Study

A grid forming converter, based on a virtual

synchronous machine (VSM) topology is represented in the three modelling techniques [14] [15].

The full modelled system is a VSM converter connected to an infinite bus through an LC filter. The power measurement is calculated from the measured AC voltage and current at the point of common coupling (PCC) and controlled to the reference power through the swing equation,

$$P_m - P_e = \frac{Jd\omega}{dt} + D\omega \quad (1)$$

with the damping, D , and inertia, J , set following the parameters given in Table I. The control of the converter is the second order implementation of the VSM swing equation, with the power directly relating to the angle set by the controller creating the power synchronization. The AC voltage is maintained by a PI controller which sets the magnitude of the voltage, which is fed into the averaged model of the converter to return the converter side voltage. This converter control was implemented in a nonlinear EMT model in Simulink, to obtain the accurate, detailed baseline to compare the other models against.

The system and control diagram are shown in Figure 1, with the direction of current considered from the converter to the grid, modelled in the dq reference frame with the d axis aligned to the a-axis, and the q axis leading 90° to it. The grid, PCC, and converter voltages are $E_g \angle 0$, $U_{PCC} \angle \theta_U$ and $V \angle \theta_V$. The grid and converter side impedances are R_n, L_n , and R_c, L_c , respectively.

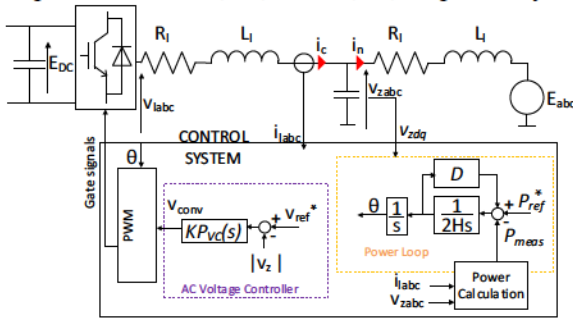


Figure 1: Virtual synchronous machine to grid connection

Small Signal Model

Following the EMT implementation of the VSM converter, a small signal model (SSM) was derived to compare to the time domain and for comparison with later models. The method of creating the SSM requires the linearization of each system component, representing the system equations in state space form, and observing the response to a small input disturbance. An

overview of the linearised systems with the defined state variables is shown in Figure 2.

TABLE I: PARAMETERS OF THE SYSTEM

Parameter	Value
Base Power, S_{base}	350 MVA
Nominal Voltage, V_n	230 kV
Grid Frequency, ω_n	50 Hz
Grid Resistance, R_n	$\frac{0.1}{SCR}$ pu
Grid Inductance, L_n	$\frac{1}{SCR}$ pu
Converter Impedance, R_c	0.01 pu
Converter Inductance, L_c	0.08 pu
Inertia Constant, H	5 s
Converter Damping pu, K_D	$2\zeta\sqrt{K_s 2H\omega_0}$
Voltage Proportional gain, K_{vp}	0.1
Voltage Integral gain, K_{vi}	50

The electrical system was linearized from the state space models; the full description of equations can be observed in [12] with the state space matrices representing the full system in the dq reference frame.

The voltages obtained from the voltage controller are passed through the linearised reference frame transformation to transform from the converter frame to the grid frame [12]. The full EMT SSM considers the dynamics of the network, the full converter impedance, and the filter capacitor ensuring full detail of the represented system.

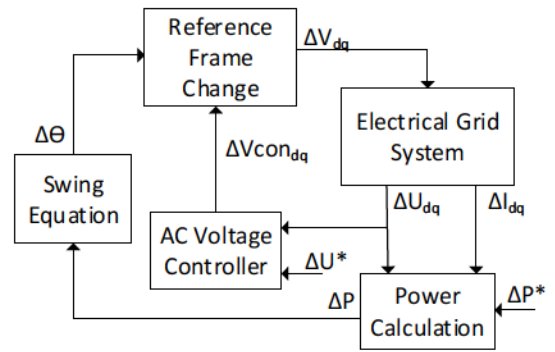


Figure 2: Linearised Small Signal Model System Connections

Jacobian Model

The static Jacobian matrix has traditionally been utilized for power flow and voltage stability analysis, despite the latter being a dynamic phenomenon. However, [13] argues that the Jacobian can still be used to observe the system dynamics if the frequency range is “quasi-static”. The Jacobian transfer matrix is based on the four transfer functions between input angle change

and input voltage change, to output power and PCC voltage change [13]. The matrix represents the AC network and the vector control of VSCs connected to the grid. It is derived from the voltage and current equations from the grid to converter circuit, represented in the dq frame, and substituting the linearised equations into the state space dq representation of the power equation [13]. However, in certain parts of the equation substitution, the resistance is neglected to simplify the equations, and this representation with the transfer functions neglects the filter capacitor and so its dynamics.

The relationship between the power, angle, and voltage, resulting in the Jacobian matrix

$$\begin{bmatrix} \Delta P \\ \Delta U \end{bmatrix} = \begin{bmatrix} J_{P\theta} & J_{PV} \\ J_{U\theta} & J_{UV} \end{bmatrix} \begin{bmatrix} \Delta\theta \\ \Delta V \end{bmatrix} \quad (2)$$

With each J_{XX} , being the derived transfer function relating each variable from the equations of the system and contain the grid dynamics representing the inputs to outputs in the Laplace transform [13]. Each of these transfer functions contain dynamic information of the converter to grid model; such detail is lacking in the next model implementation.

Classical 2nd Order Model

The simplest representation of a virtual synchronous machine connected to an infinite bus involves the swing equation and synchronising torque coefficient [7], as shown in Figure 3. The swing equation is the same VSM control structure used in the full EMT SSM and the Jacobian model. In the Classical model however, the grid is represented only by the synchronising torque, K_s . The electromagnetic torque can be separated into the synchronising torque and the damping torque, with their coefficients defined by K_s [pu torque/ radians] and K_d [pu torque/pu speed deviation] respectively. The coefficient K_s is defined by

$$K_s = \frac{EV}{X_T} \cos(\delta_0) \quad (3)$$

and takes into account the infinite bus voltage, synchronous machine output voltage, reactance between the two and the angle difference. The damping coefficient is calculated by

$$K_D = 2\zeta\sqrt{K_s 2H\omega_0} \quad (4)$$

where ζ is the damping ratio. However, (3) does not take into consideration the resistance between the infinite bus and synchronous machine, and is based on algebraic equations so lacks any related dynamic information [16]. The synchronising torque coefficient indicates system

stability, with a negative value showing unstable non-oscillatory modes, and negative damping torque coefficient indicating unstable oscillatory modes [17].

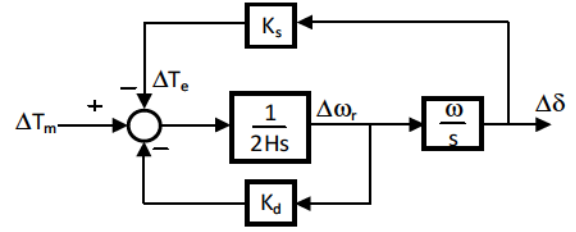


Figure 3: Basic Virtual Synchronous Machine Control Model

The limitations of this model depend on what information is required. There are several higher order and more complex control structures of the VSM, however they can be difficult to use for analytical dynamic analysis. The “importance” of some of the electromagnetic phenomena has also been debated in the literature [18], the relevance of the neglect of electromagnetic dynamics is less clear in the presence of converter interfaced generation. The full small signal and Jacobian models have cross coupling terms representing the dynamics of the impedances which are not included in the classical model. This is a significant limitation of the basic Classical model, and the impact of this can be observed in the results section with the reduction in X/R ratio.

Results

Overview of Step Response

The increase in power converter connected devices and the change in site generation geographical location is resulting in several changes in the grid, namely in SCR and X/R ratio [3]. Most control structures of grid connected power converters are grid following, which have a high impedance and so this is reducing the SCR of the grid in certain areas. The distribution grid is now experiencing areas of significantly low SCR, and low X/R ratio. Therefore, it is important to represent the effect of these changing parameters on the models’ accuracy.

A series of parametric sweeps were performed on each of the models to investigate the effect of short circuit ratio, damping ratio, ζ , and X/R ratio on the accuracy of the models. A step input of 0.03 pu power (10 MW) is observed for each model as the first case study.

The higher the X/R ratio, the greater the decoupling between active and reactive power [4] and so a step in the reference power should

control the measured power without significant effect on the voltage. However, decreasing the X/R ratio results in the classical model and Jacobian models having reduced accuracy. For the Classical model, this is due to the lack of representation of voltage control dynamics. This can be observed between Figure 4 a and b, where the X/R ratio is reduced from 10 to 5, at SCR of 1.5, and the Classical model loses accuracy slightly, but not significantly. Further reducing the X/R ratio to 1 shows significant error in both the classical and Jacobian models, deviating from the EMT model, showing longer lasting oscillations.

The effect of reducing the X/R ratio is most critical at lower SCRs. If the SCR is increased

from 1.5 to 6, for the same X/R=1 and $\zeta=0.1$, the Jacobian and Classical model match the time domain model slightly better than at the lower SCR. The model can suitably represent small changes around the equilibrium point, however lower SCRs and X/R ratios result in larger inaccuracies. Furthermore, this Classical model cannot reflect the changes in voltage reference as the voltage control loop is not included in the model. With the lower SCR, the frequency of the oscillations differs for the Jacobian and Classical models, compared to each other and the EMT, resulting in the waveforms being out of phase with each other.

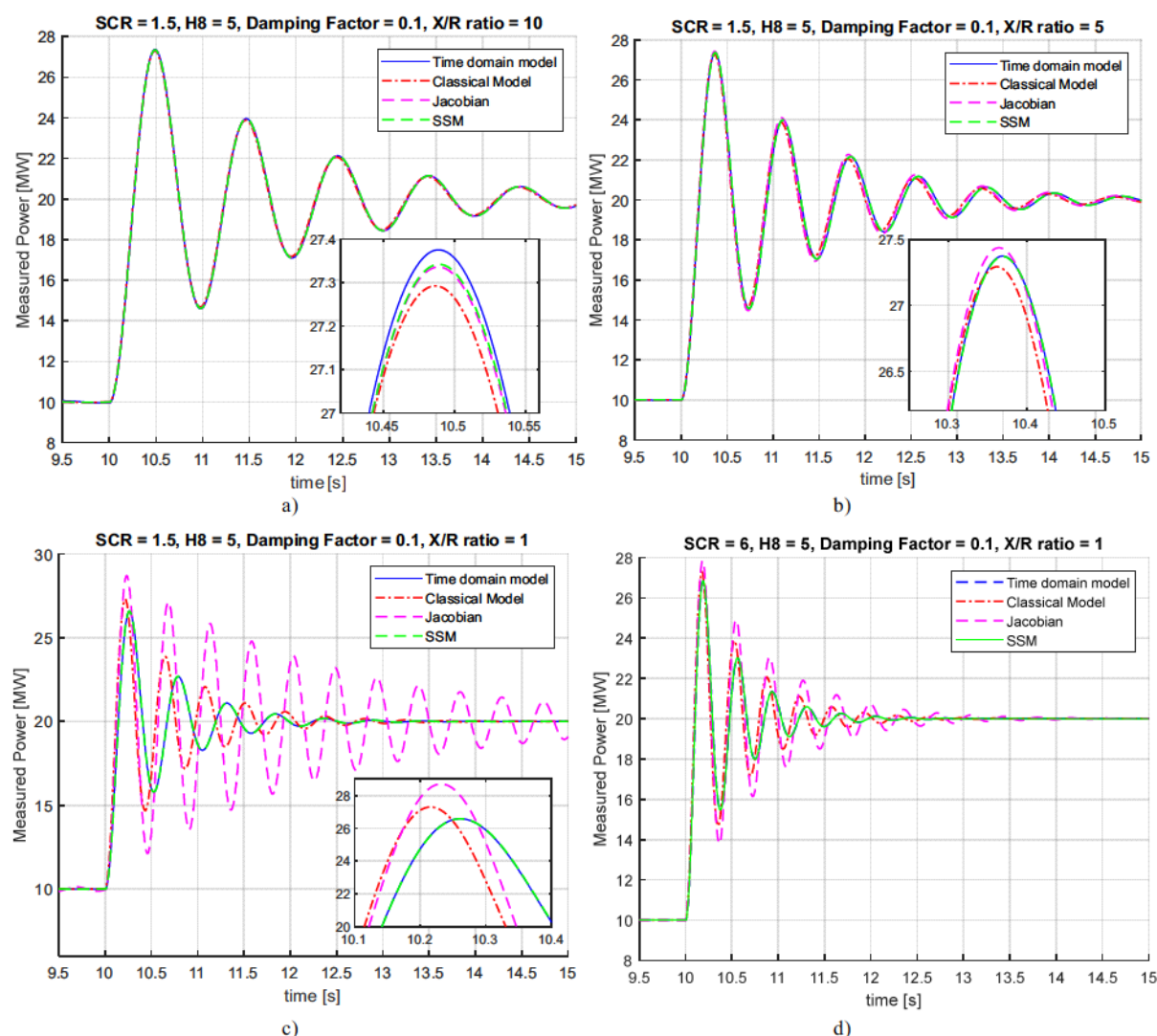


Figure 4: Step of 10 MW (0.03pu) SCR = 1.5, $\zeta = 0.1$ a) X/R = 10; b) X/R = 5; c) X/R = 1; d) SCR = 6, $\zeta = 0.1$, X/R = 10

Eigenvalue Analysis

For the full range of investigated SCRs, X/R ratios and damping ratios, the full EMT SSM model completely matched the nonlinear EMT

model. Therefore, the eigenvalues of the full SSM model will be used as the accuracy baseline for the model small signal comparisons. For the same parameters investigated, the eigenvalues were analysed. The voltage controller and network modes are represented by the full SSM and the

Jacobian models, but they are much more heavily damped than the electromechanical modes and so will be damped out much faster. This can be seen in Table II, where the full range of the real parts of the eigenvalues are shown but the electromechanical modes are emphasized in bold. Therefore, only the electromechanical modes will be analysed for comparison.

TABLE II: REAL COMPONENTS OF EIGENVALUES OF MODELS: SCR = 1.5, $\zeta = 1$, X/R = 10

<i>Full SSM</i>	<i>Jacobian</i>	<i>Classical</i>
± 0.6339	± 0.6358	± 0.6486
± 12.4488	± 30.9007	
± 32.2373	± 32.2574	
-41.2439	-41.0783	
± 5.3926		

For a constant SCR of 1.5, and damping ratio of 0.1, the X/R ratio was reduced from 10 to 1, with modes for each model shown in Figure 5. As the X/R ratio is decreased, the electromechanical modes become more damped for the Classical and full SSM models, but the Classical and Jacobian modes move further apart in frequency (imaginary axis) from the full SSM model, causing them to become out of phase with each other and the full SSM model. They also deviate in terms of damping (time constant), due to the deviations in the real axis.

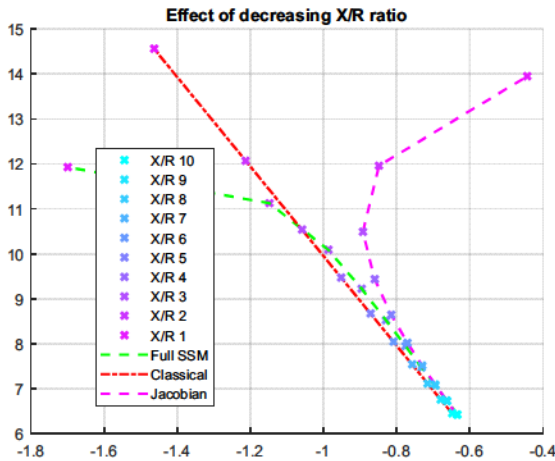


Figure 5: Comparison of the models with SCR 1.5, ζ 0.1, $H = 5$ s, over decreasing X/R ratio (10 to 1)

Towards the lower end of the X/R ratio range, the Jacobian modes are significantly different from the full SSM electromechanical modes, which was observed in the oscillations of the

model in Figure 4c. The modes of each model begin to significantly diverge from each other from $X/R < 3$. Increasing the SCR, at a low X/R ratio, results in the modes becoming more damped again but with closer together frequencies and so this phase shifting is not as pronounced.

Model Comparison Overview

The limits of the converter modelling methods in regards to accuracy are subjective in a sense. The small signal model matches the EMT model incredibly well for the full range of investigated parameters, SCR, damping ratio and X/R ratio. For high X/R ratios, the Classical and Jacobian models follow the EMT response very well for SCRs greater than 3 and damping factors greater than 0.3. For the lower X/R ratio of 1, SCR 6, the initial response is acceptable but begins to get out of phase, and deviate in terms of damping. Also, as the SCR is reduced, these models begin to lose accuracy significantly for all damping ratios.

The general conclusions of the effect of the parameters on model accuracy can be displayed in the heatmaps of Figure 6 and Figure 7. For the three modelling techniques, the system was implemented as a linear time-invariant block with the corresponding state space system selected, and the output of each compared to the EMT model. The sum of the squares of the error for each point of the response after the step was then calculated compared to the EMT response following

$$\% \text{ Error} = 100 \sqrt{\frac{\sum_{i=0}^n (P_{mi} - P_{sim_i})^2}{\sum_{i=0}^n P_{sim_i}^2}} \quad (5)$$

Where P_{sim} is the EMT Simulink response at point i , and P_m is the investigated model at time i .

Therefore, Figure 6 and Figure 7 are heatmaps to show for each modelling technique, the percentage error in accuracy compared to the EMT time domain model, across the parameters investigated.

For the range of SCRs and damping ratio, the sum of the squares of the error was calculated for each X/R ratio. For the X/R ratio of 10, Figure 6, the greatest error was with the classical model at SCR 5 and damping ratio of 0.1. The exact percentage error of this value is only 0.72%, which is very insignificant. Considering this is the highest error for this parametric sweep, the other errors for the remaining models, SCRs and ζ , are even smaller and so show great accuracy. As the overall error is very small, for a small signal power disturbance, any three of the models would

be capable of accurate representation, and the classical model has the lowest computational burden and so could be used very effectively for this type of investigation for the given parameters.

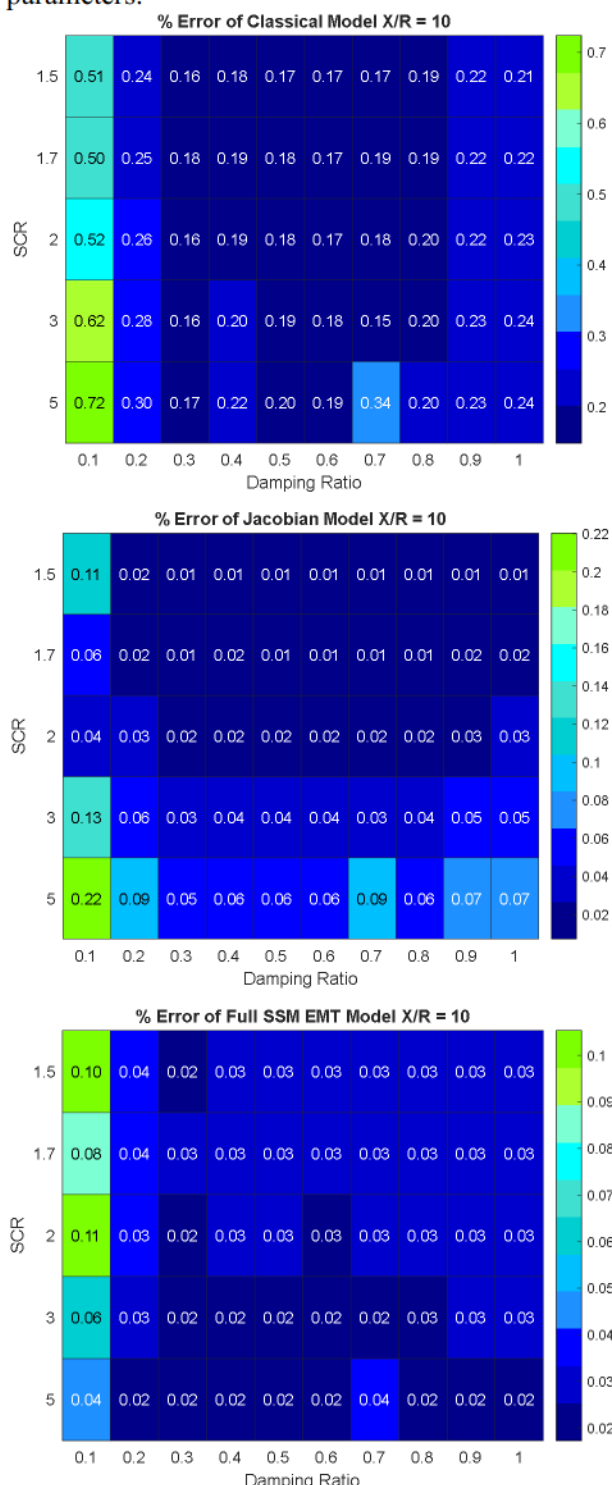


Figure 6: Percentage Error Heatmaps of Model Accuracy for X/R = 10; a) Classical; b) Jacobian; c) Full SSM

When the X/R ratio is reduced to 1, a significant change is observed in the accuracy of the Classical and Jacobian models, shown in heatmaps of Figure 7.

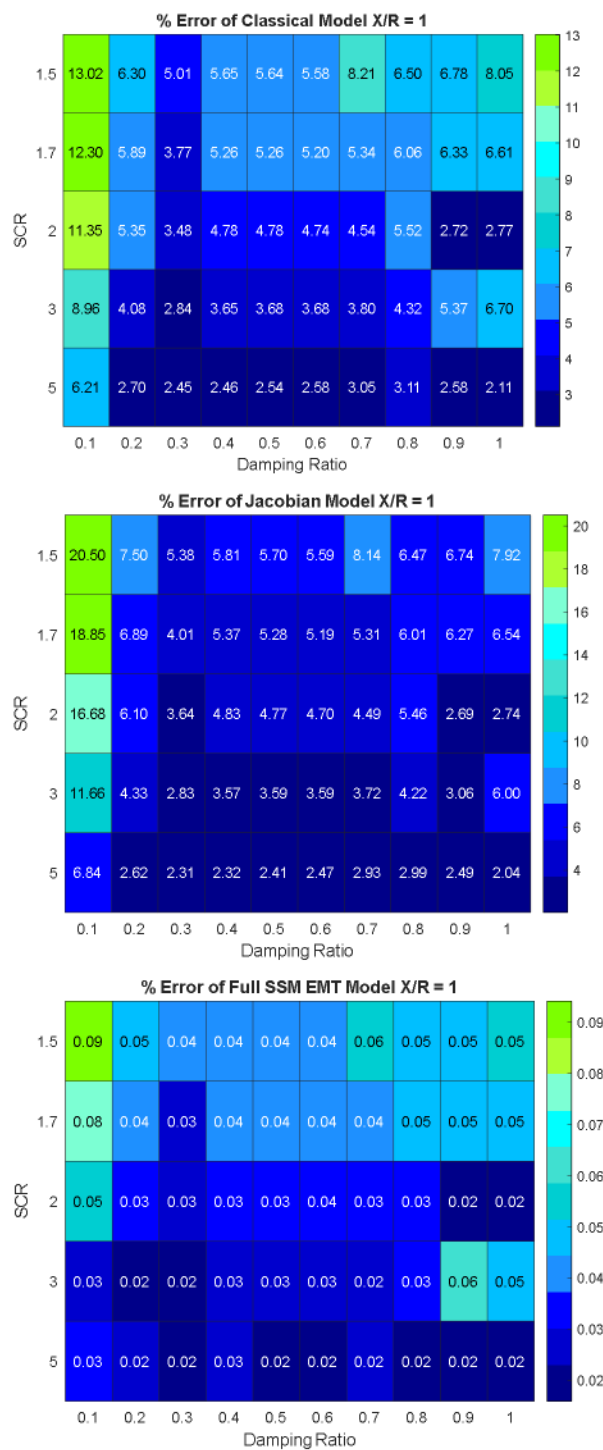


Figure 7: Percentage Error Heatmaps of Model Accuracy for X/R = 1; a) Classical; b) Jacobian; c) Full SSM

The greatest error is observed in the Jacobian model at SCR 1.5 and damping 0.1 of 20.5%. For the classical model with the aforementioned parameters, the error is 13%, and for the full EMT SSM, the error is only 0.09%. For the Jacobian and Classical models at this X/R ratio of 1, across all SCRs and damping ratios the percentage error is significantly increased compared to the same parameters but with a higher X/R. The EMT SSM

however still maintains a very good accuracy across all parameters.

The Jacobian model can accurately represent the dynamic response of a power step with an $X/R > 3$, as seen in the graphs of Figure 5 to Figure 7. However, at lower X/R ratios, the response is increasingly inaccurate, especially at $SCR < 2$ and $\zeta < 0.2$. The Classical model has the same limitations for each parameter. Therefore, between the Jacobian and Classical models there is not much of a difference between the limits of accuracy dependent on parameters. The EMT SSM is accurate in all instances, and fully matches the nonlinear EMT, and the classical and Jacobian models could be sufficient in representing a power step change with $X/R > 3$.

Conclusion

The modelling of converter dominated networks, and identification of interactions within, is becoming increasingly complex. As such, maintaining the balance between accurate, detailed models, and an appropriate computational burden is paramount. Nonlinear EMT modelling provides the most accurate response, yet is limited by having the highest computational cost, and the full small signal model is incredibly useful for converter interaction and sub-synchronous oscillation analysis however at a high complexity with limited scalability. Simplified models such as the Jacobian representation or the classical second order model allow for simple analysis but do not always appropriately show the dynamics of the grid/converter, and at lower SCRs and non-moderate damping ratios, they show an increased error, especially at lower X/R ratios. For the range of short circuit ratios of 2 to 6, and damping ratios of 0.1 to 1, the classical and Jacobian models are as accurate as a full small signal model, when at a high X/R ratio. However, with an $X/R < 3$, the Jacobian and Classical models have a much lower accuracy compared to the full EMT SSM, especially at $SCR < 2$ and damping ratio < 0.2 . The inclusion of the full converter to grid impedances as well as filter capacitance is key for The EMT Small signal model includes the grid and converter side impedances and the filter capacitor. The Classical model only includes the equivalent inductance between the grid and converter, ignoring the resistance and capacitance. The Jacobian model mainly considers the grid

impedance, but makes some simplifications in some of the internal transfer functions by neglecting the grid resistance in some cases. These simplifications allow for ease of implementation but result in lack of dynamic detail and damping. These limitations of the Jacobian and Classical model result in significantly reduced accuracy for the increasingly seen “extreme” grid parameters.

References

- [1] ENTSO-E, “High Penetration of Power Electronic Interfaced Power Sources and the Potential Contribution of Grid Forming Converters,” p. 61, 2019, [Online]. Available: https://www.entsoe.eu/Documents/Publications/SOC/High_Penetration_of_Power_Electronic_Interfaced_Power_Sources_and_the_Potential_Contribution_of_Grid_Forming_Converters.pdf
- [2] R. N. Damas, Y. Son, M. Yoon, S.-Y. Kim, and S. Choi, “Subsynchronous Oscillation and Advanced Analysis: A Review,” *IEEE Access*, vol. 8, pp. 224020–224032, 2020, doi: 10.1109/ACCESS.2020.3044634.
- [3] B. Zhao, R. Zeng, Q. Song, Z. Yu, and L. Qu, “Medium-voltage DC power distribution technology,” in *The Energy Internet: An Open Energy Platform to Transform Legacy Power Systems into Open Innovation and Global Economic Engines*, W. Su and A. Q. Huang, Eds. Woodhead Publishing, 2019, pp. 123–152. doi: 10.1016/B978-0-08-102207-8.00006-0.
- [4] B. Shao *et al.*, “Power coupling analysis and improved decoupling control for the VSC connected to a weak AC grid,” *International Journal of Electrical Power & Energy Systems*, vol. 145, p. 108645, 2023, doi: <https://doi.org/10.1016/j.ijepes.2022.108645>.
- [5] G. Misyris *et al.*, “North Sea Wind Power Hub: System Configurations, Grid Implementation and Techno-economic Assessment,” APA, 2020.
- [6] G. S. Misyris, S. Chatzivasileiadis, and T. Weckesser, “Grid-forming converters: Sufficient conditions for RMS modeling,” *Electric Power Systems Research*, vol. 197, p. 107324, 2021, doi:

- <https://doi.org/10.1016/j.epsr.2021.107324>.
- [7] P. Kundur, *Power System Stability And Control*. Toronto: McGraw-Hill Professional, 1994.
- [8] V. D. E. F. N. N. Guideline, “VDE FNN Guideline FNN Guideline : Grid forming behaviour of HVDC systems and DC-connected PPMs”.
- [9] N. Hatziargyriou *et al.*, “Definition and Classification of Power System Stability – Revisited & Extended,” *IEEE Transactions on Power Systems*, vol. 36, no. 4, pp. 3271–3281, 2021, doi: 10.1109/TPWRS.2020.3041774.
- [10] X. Wang and F. Yang, “Equivalent simplification of torsional dynamics in the closely coupled identical turbine-generators,” *2006 IEEE Power Engineering Society General Meeting, PES*, pp. 13–16, 2006, doi: 10.1109/pes.2006.1708851.
- [11] Y. Fan, W. Xitian, X. Yingxin, and C. Chen, “Dynamic equivalence of torsional interaction in multi-identical-machine power system,” *Electric Power Components and Systems*, vol. 35, no. 5, pp. 525–537, 2007, doi: 10.1080/15325000601078161.
- [12] A. Egea-Alvarez, S. Fekriasl, F. Hassan, and O. Gomis-Bellmunt, “Advanced Vector Control for Voltage Source Converters Connected to Weak Grids,” *IEEE Transactions on Power Systems*, vol. 30, no. 6, pp. 3072–3081, 2015, doi: 10.1109/TPWRS.2014.2384596.
- [13] L. Zhang, L. Harnefors, S. Member, and H. Nee, *Modeling and Control of VSC-HVDC Links Connected to Island Systems*. 2010.
- [14] H. Bevrani, T. Ise, and Y. Miura, “Virtual synchronous generators: A survey and new perspectives,” *International Journal of Electrical Power and Energy Systems*, vol. 54, pp. 244–254, 2014, doi: 10.1016/j.ijepes.2013.07.009.
- [15] Y. Gu and T. C. Green, “Power System Stability With a High Penetration of Inverter-Based Resources,” *Proceedings of the IEEE*, pp. 1–22, 2022, doi: 10.1109/JPROC.2022.3179826.
- [16] G. de Carne *et al.*, “Which Deepness Class Is Suited for Modeling Power Electronics?: A Guide for Choosing the Right Model for Grid-Integration Studies,” *IEEE Industrial Electronics Magazine*, vol. 13, no. 2, pp. 41–55, Jun. 2019, doi: 10.1109/MIE.2019.2909799.
- [17] A. Hammoudeh, M. I. al Saaideh, E. A. Feilat, and H. Mubarak, “Estimation of Synchronizing and Damping Torque Coefficients Using Deep Learning,” in *2019 IEEE Jordan International Joint Conference on Electrical Engineering and Information Technology (JEEIT)*, 2019, pp. 488–493. doi: 10.1109/JEEIT.2019.8717432.
- [18] J. Ritonja, M. Petrun, J. Cernelic, R. Brezovnik, and B. Polajžer, “Analysis and Applicability of Heffron–Phillips Model,” *Elektronika ir Elektrotehnika*, vol. 22, Dec. 2016, doi: 10.5755/j01.eie.22.4.15905.